ACS Sustainable Chemistry & Engineering

Research Article

pubs.acs.org/journal/ascecg

Sustainable Processing and Synthesis of Nontoxic and Antibacterial Magnetic Nanocomposite from Spider Silk in Neoteric Solvents

Nripat Singh,[†,‡] Dibyendu Mondal,[†,‡] Mukesh Sharma,[†,‡] Ranjitsinh V. Devkar,[∥] Sonam Dubey,[‡,§] and Kamalesh Prasad*[,†,‡]

[†]Marine Biotechnology and Ecology Division, CSIR-Central Salt & Marine Chemicals Research Institute, G. B Marg, Bhavnagar, 364002 Gujarat, India

[‡]AcSIR-Central Salt & Marine Chemicals Research Institute, G. B Marg, Bhavnagar, 364002 Gujarat, India

[§]Salt & Marine Chemicals Division, CSIR-Central Salt & Marine Chemicals Research Institute, G. B Marg, Bhavnagar, 364002 Gujarat, India

[∥]Division of Phytotherapeutics and Metabolic Endocrinology, Department of Zoology, Faculty of Science, The M.S. University of Baroda, Vadodara, 390002 Gujarat, India

Supporting Information

ABSTRACT: Different neoteric solvents (both ionic liquids and deep eutectic solvents) were used for the dispersion and preparation of bionanocomposite of spider silk fibers (*Crossopriza lyoni*). Among these solvents, hydrated tetrabutylammonium hydroxide was found to disperse 7.5 mg mL^{-1} of spider silk with nanoscale structural distribution at room temperature. Analyses of the regenerated spider silk from the solution indicated preservation of the chemical structures of the protein blocks in the fibers during the dispersion process. The quaternary ammonium based IL was further used as dispersion media for the fabrication of Fe_3O_4 functionalized bionanocomposite. Attachment of Fe_3O_4 nanoparticles on the spider silk surfaces and preservation of the chemical structures of the protein blocks of the spider silk in the composite was also established. The materials generated do not appear to inhibit the growth of mammalian cells *in vitro* and showed antibacterial properties and thus demonstrate their potential for therapeutic applications.

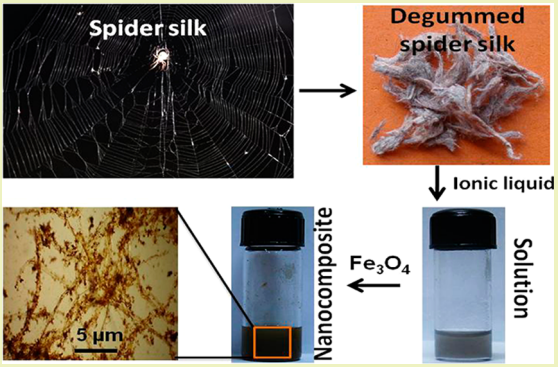

KEYWORDS: *Neoteric solvents, Spider silk fibers, Nanoscale dispersion, Bionanocomposite, Cytotoxicity, Antibacterial activity*

INTRODUCTION

Proteins are one of the most important biomacromolecules found in living systems and play a key role in all biological processes such as mechanical support, immune protection, enzymatic catalysis, and control and differentiation of the cells and tissues and hence attracting considerable interest in the preparation of functional biomaterials useful in many fields such as drug delivery, tissue regeneration, biosensors, etc.[1,2] Among proteins, natural silk fibers associated with unique physical and chemical properties similar to those of many of the synthetic fibers are of interest.[3] Among the various naturally available silk fibers, the spider silk fibers (SSF) have attracted interest for thousands of years due to their unusual toughness and ductility.[4] Chemically, SSF is a polypeptide consisting of proteins that possess large quantities of nonpolar and hydrophobic amino acids such as glycine and alanine with traces of other amino acids such as glutamine, serine, leucine, valine, proline, tyrosine, and arginine. Certain biomaterials have demonstrated outstanding properties even better than several man-made materials. Spider silk is one such material evolving as an outstanding fibrous proteinous biomaterial with tensile strength of about 1.65 GPa and elasticity equivalent to many nylon based commercially available materials (such as Kevlar).[5,6] In addition to the excellent mechanical properties, the SSF show biocompatibility, cell adhesion, and biodegradability making them useful in biomedical applications.[1,2] Other silk fibers such as those obtained from *Bombyx mori* silk worms are found to form thixotropic hydrogels suitable to be used as injectable hydrogels.[7]

To make the SSFs useful for large scale applications, the processing of the fibers plays a vital role. In the wet spinning method of processing, hexafluoro-2-propanol is used as a solvent to dissolve the fibers and polar solvents like methanol, isopropyl alcohol, and acetone are used as coagulants. All the wet spinning methods developed so far consist of multiple steps, and a tedious pretreatment stage and use of toxic solvents also made many of the processes unattractive for commercial exploitation.[8−10] Easier solvent systems consisting of a mixture

Received: August 4, 2015
Revised: September 4, 2015
Published: September 9, 2015

DOI: 10.1021/acssuschemeng.5b00810
ACS Sustainable Chem. Eng. 2015, 3, 2575−2581

Table 1. Optimization Process for the Preparation of Nanoscale Dispersion of Spider Silk Fibers Using ILs/DESs[a]

entry	IL/DES	SSF amount (mg·mL^{-1})	temperature (°C)	observation and time
1	TBAH (40% in water)	5	r.t.	D, 2 h
2		7.5	r.t	D, 10 h
3		10	r.t.	PD, 12 h
3	TBAA	1	r.t. to 120[b]	ND, 12 h
4	Cho-Gly	1	r.t. to 120[b]	ND, 12 h
5	Cho-formate	1	r.t. to 120[b]	ND, 12 h
6	ChoCl−urea (l:2)	1	r.t. to 120[b]	ND, 12 h
7	ChoCl−EG (1:2)	1	r.t. to 120[b]	ND, 12h

[a]r.t. = room temperature (25 °C); D = Dispersed; PD = partially dispersed; ND = Not dispersed. [b]= maximum temperature.

of acid and salts are used to dissolve silk fibers (*Bombyx mori*) and regeneration on the nanofibril scale.[11] Such silk fibers were used to prepare composite materials with Fe_3O_4 for delivery of cancer therapeutics, magnetic material after uniform coating with Fe_3O_4.[12−14] Preparation of biopolymers based materials demands effective dissolution of the polymers in solvents for further processing. Because of the H-bonded β-sheet nanocrystals embedded in a semiamorphous protein domain, spider silk is difficult to dissolve in common solvents and is also resistant to acid treatment. In addition to the above-mentioned solvents to dissolve the fibers, attempts have been made to produce spider silk based protein nanocomposites and nanofibers by hydrolysis with concentrated sulfuric acid. Besides the hazardousness of the process, acid treatment did not affect the β-sheet structure and thus further processing requires several other chemical/enzymatic treatments.[15]

Super critical fluids and ionic liquids (ILs) are considered as neoteric solvents in "green chemistry" and are emerging as an alternative to many of the conventional solvents.[16] The unique dissolution capabilities of ILs and their structural analogues, known as deep eutectic solvents (DESs), make them one of the most suitable solvents for the processing of biopolymers including proteins.[17−19] These solvents were also successful in dissolving biopolymers such as chitin and DNA.[20−22] Dissolution and regeneration of *Bombyx mori* silk fibers in imidazolium based ILs having different anions were investigated, and it was found that the anions play an important role in the dissolution of the fibers.[23] Use of protic ionic liquids was reported to produce silk fibroin with tunable properties.[24]

Herewith we have investigated the nanoscale dispersion and regeneration of spider silk fibers obtained from the webs of spiders (genus, *Crosspriza*; family, *Pholcidae*) commonly known as box spiders, which are found almost in all tropical regions and are harmless to humans.[25] The silk fibers were further used to prepare magnetic nanocomposite materials having antibacterial (against both Gram positive and negative) and noncytotoxic properties (against human lung carcinoma cells) using the suitable IL. Preservation of the chemical structure of the protein blocks present in the silk fibers during dissolution and composite formation was also investigated.

EXPERIMENTAL SECTION

Materials. Tetrabutylammonium hydroxide (TBAH, 40 wt % in water) and tetrabutyl ammonium acetate (TBAA) were purchased from TCI Chemicals, Tokyo, Japan. Choline bicarbonate was purchased from Sigma-Aldrich, USA. $FeCl_3{\cdot}6H_2O$ and $FeSO_4{\cdot}7H_2O$ were purchased from SISCO Research Laboratories Pvt. Ltd., Mumbai, India. Choline chloride, formic acid, ethylene glycol, and isopropyl alcohol (IPA) were purchased from SD Fine Chemicals, Mumbai, India. Urea was purchased from RFCL Ltd., New Delhi, India. NaOH and $NaHCO_3$ were procured from Central Drug House (P) Ltd., New Delhi, India. All chemicals were of analytical grade and used as received.

About 10 g of spider silk fibers (SSF) was collected from naturally accumulated locations in the laboratory building (21.7600° N, 72.1500° E). Collected SSF were washed with water for several times to remove the dust prior to their degumming and nanoscale dispersion followed by preparation of the nanocomposite. Choline glycolate and choline formate were prepared by the simple metathesis reaction between choline bicarbonate and glycolic acid or formic acid in equimolar ratio.[26] Deep eutectic solvents were obtained by the complexation of choline chloride and urea in 1:2 molar ratio (ChoCl−Urea 1:2) or ethylene glycol in 1:2 molar ratio (ChoCl−EG 1:2) as reported earlier.[27]

Degumming of Spider Silk Fiber. Because the naturally collected spider silk was very gummy in nature (Figure S1), degumming of spider silk was carried out following the process reported by Kim et al. (2003).[28] In a typical process, freshly collected spider silk was washed with distilled water for several times to remove dust particles followed by degumming twice with 0.5% w/v of sodium bicarbonate ($NaHCO_3$) aqueous solution at 100 °C for 30 min. The degummed SSF thus obtained was washed with hot distilled water for several times and lyophilized to obtain dry degummed SSF (DSSF).

Synthesis of Fe_3O_4 Particles. For the synthesis of Fe_3O_4, 5.4 g of $FeCl_3{\cdot}6H_2O$ and 3.6 g of urea were dissolved in 200 mL of deionized water at 90 °C for 2 h. The mixture was kept at room temperature for cooling. Subsequently, 2.8 g of $FeSO_4{\cdot}7H_2O$ was added to this mixture and the pH was adjusted to 10 by dropwise addition of NaOH (0.1 M) solution with continuous stirring. Black precipitates of iron oxide appeared, which were ultrasonicated for 30 min. The mixture was kept at room temperature for a few hours without any disturbance to complete the coagulation of the black precipitates. The resulted precipitate was washed with deionized water for several times and vacuum-dried.[29]

Nanoscale Dispersion and Regeneration of Degummed SSF. For the nanoscale dispersion of SSF, 1−10 mg of DSSF was added to a vial containing 1 g of ionic liquid (IL) or deep eutectic solvent (DES) followed by stirring in the temperature range from room temperature to 120 °C until the complete dispersion of SSF in ILs/DESs (Table 1). No dispersion was considered when the addition of 1 mg SSF in 1 mL IL/DES appeared cloudy. The SSF in the dispersed solutions was regenerated by adding the dispersion in excess isopropyl alcohol (IPA) and termed as RSSF.

Preparation of Magnetic SSF. The magnetic SSF was prepared using TBAH as dispersion media. In a typical reaction, 5 mg of degummed SSF was added in a vial containing 1 mL of TBAH and the mixture was stirred at room temperature for 2 h (optimized duration) to obtain dispersion of SSF followed by the addition of 5 mg of Fe_3O_4 powder and ultrasonication at room temperature for 30 min. The Fe_3O_4 functionalized SSF was washed with water for several times and lyophilized to get a dry powder.

Characterization. Degummed SSF and functionalized SSF along with their regenerated counterparts were characterized by employing various analytical instruments. FT-IR was recorded on a PerkinElmer FT-IR machine (Spectrum GX, GSA) using a KBr disc. The powder X-ray diffraction (XRD) patterns were recorded at 298 K on a Philips X'pert MPD System using Cu Kα radiation (λ = 0.154 05 nm) with 2θ

DOI: 10.1021/acssuschemeng.5b00810
ACS Sustainable Chem. Eng. 2015, 3, 2575−2581

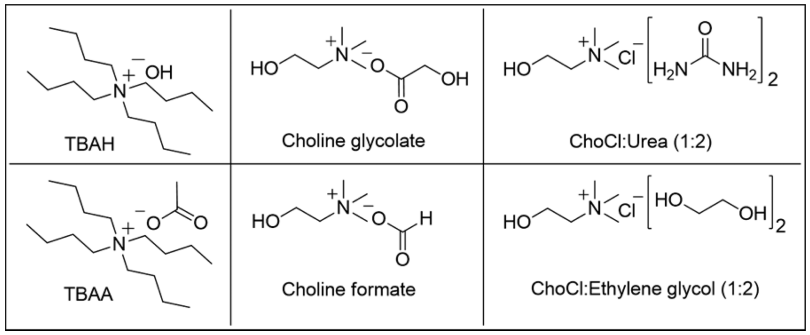

Figure 1. Structure of neoteric solvents used for the dispersion and preparation of nanocomposite of spider silk fibers.

Scheme 1. Photographic Representation for the Nanoscale Dispersion of Degummed Spider Silk Fibers in Hydrated TBAH and Preparation of Magnetic Bionanocomposite

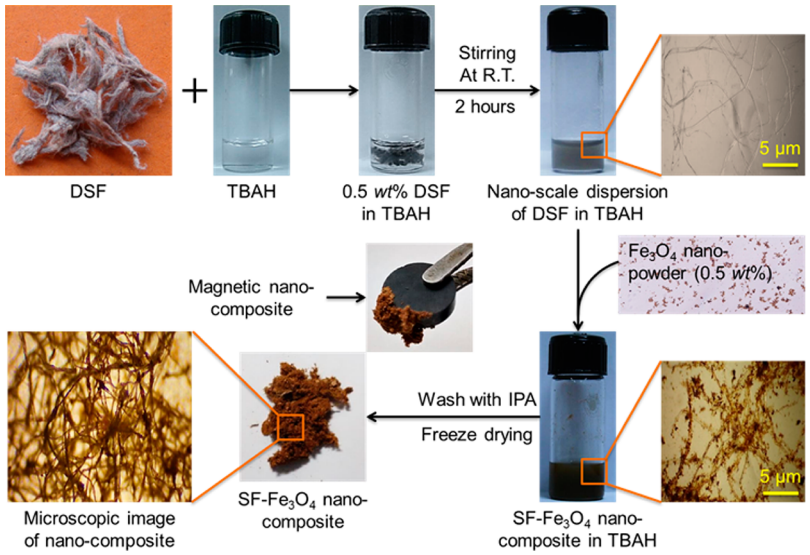

= 5°−80° at a scan speed of 0.1° s^{-1}. Thermo gravimetric analysis (TGA) was carried out on a NETZSCH TG 209F1 Libra TGA209F1D-0105-L machine using a temperature programmer 30−500 °C at a heating rate 5 °C min^{-1} under nitrogen gas atmosphere. Differential scanning calorimetry (DSC) was measured on a NETZSCH DC 209F1 Libra DCA209F1D-0105-L machine using a temperature range of −80 to +160 °C at a heating rate 5 °C min^{-1} under nitrogen gas atmosphere. The dispersion of pure SSF and its functional derivative was monitored using optical light microscope with 100× magnification (Fine Vision Microscope, India). Field emission-scanning electron microscopy (FE-SEM) images were recorded on a JEOL JSM-7100F instrument employing 18 kV accelerating voltage. Atomic force microscopy (AFM) images were recorded in semicontact mode using a NTEGRA NT-MDT TS-150 instrument, Russia. Viscosity was measured on a Brookfield DV-II + Pro viscometer at 25 °C at 140 rpm using spindle SC4-18. Electrospray-mass spectrometry (ESI-MS) measurements were carried out on a Q-TOF micro mass spectrometer (USA), equipped with an electrospray ionization source, time-of-flight (TOF) analyzer and microchannel plate (MCP) detector.

Cytotoxicity Analyses. *Cell Line and Culture.* All the solutions used were filtered through a 0.22 μ filter (Millipore Biomedical Aids Pvt. Ltd., Pune) prior to their use for the experiment. Human lung carcinoma (A549) cells were obtained from National Centre for Cell Science, Pune, India and were incubated at 37 °C with 5% in a water jacketed CO_2 incubator (Thermo Scientific, Forma series II 3111, USA). Cells were seeded (1×10^5 cells) in a T25 flask and cultured in DMEM containing 10% FBS and 1% antibiotic−antimycotic solution. Cells were trypsinized every third day by subculturing with TPVG solution.

Cell Viability (MTT) Assay. Cytotoxic potential was determined by 3-(4,5-dimethylthiazol-2-yl)-2,5-diphenyltetrazolium bromide (MTT) assay. Cells (7×10^3 cells/well) were seeded in 96-well culture plates for 24 h and then treated with a dose range of 10, 20, 30, 40, 50, 60, 70, 80, 90, 100, and 200 $\mu g \cdot mL^{-1}$ concentrations of both the materials (SSF and magnetic SSF) for 24 h. Later on, 10 μL of MTT (5 $mg \cdot mL^{-1}$) was added followed by incubation for 4 h at 37 °C. The contents were discarded and wells washed with phosphate buffered saline (PBS). Formazan was formed at the end of this reaction and the same was dissolved in 150 μL of DMSO and absorbance was read at 540 nm using an ELX800 Universal Microplate Reader (Bio-Tek instruments, Inc., Winooski, VT) and the percentage cell viability was calculated (Thounaojam et al., 2010).[30]

Statistical Analysis. Data were analyzed for statistical significance using one way analysis of variance (ANOVA) followed by Dunnett's multiple comparison test, and the results were expressed as mean ± SEM using Graph Pad Prism version 6.0 for Windows, Graph Pad Software, San Diego, California, USA.

Antibacterial Efficacy. Bacteria were grown in Nutrient Broth and Zobell Marine broth in the presence and absence of the SSF and its magnetic derivative. Both Gram positive (*Bacillus licheniformis*) and Gram negative bacteria (*Escherichia coli* and *Pseudomonas stutzeri*) were used in the experiment. To assess the antibacterial activity SSF and its magnetic derivative, bacteria such as *Escherichia coli* and *Bacillus licheniformis* were grown initially in Nutrient Broth and *Pseudomonas stutzeri* in Zobell Marine Broth. Tubes containing these cultures were kept for incubation at 37 °C for 24 h at 120 rpm in a shaker. After

DOI: 10.1021/acssuschemeng.5b00810
ACS Sustainable Chem. Eng. 2015, 3, 2575−2581

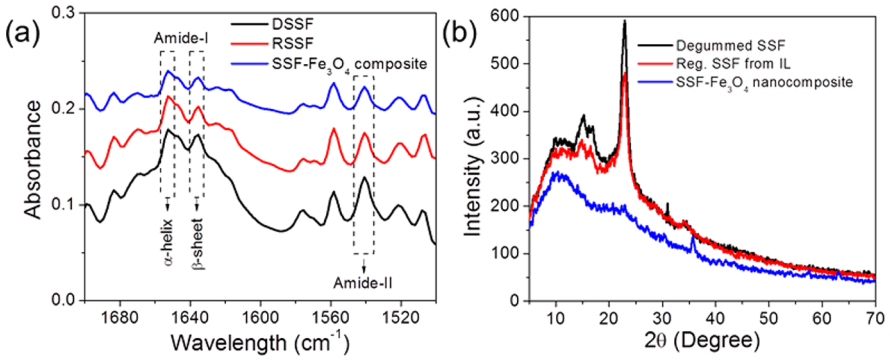

Figure 2. (a) FT-IR spectra and (b) powder XRD spectra of degummed SSF, regenerated SSF, and SSF−Fe_3O_4 nanocomposite.

incubation, 100 μL of the cultures was added to fresh media with SSF and magnetic SSF, respectively. Another tube without test material was kept as control (media + culture). Optical density was measured at 660 nm after 24 h of incubation.

RESULTS AND DISCUSSION

The ash content of the as-collected SSF was 54.28% w/w, whereas the degummed SSF showed presence of only 5.76% w/w of ash, indicating presence of a large amount of inorganic contaminants in the SSF, which were removed during the degumming process. From the elemental analysis of SSF before and after degumming, a substantial increase in the carbon content of degummed spider silk fiber was observed, which complimented the ash content data (Table S1).

The various neoteric solvents (Figure 1), such as hydrated tetrabutylammonium hydroxide (TBAH), tetrabutylammonium acetate (TBAA), choline glycolate (Chol-Glyc), choline formate (Chol-form), and two DESs obtained by the complexation between choline chloride and urea (ChoCl−urea 1:2) and ethylene glycol (ChoCl−EG 1:2) were used to dissolve degummed spider silk (DSF) maintaining different reaction parameters as summarized in Table 1. Digital photographs of the dissolution of DSF in different ILs and DESs are shown in Figure S2.

It can be observed from Table 1 that among the neoteric solvents, TBAH having 40% water could disperse DSSF up to 7.5 mg mL^{-1} at room temperature (25 °C) upon 10 h of gentle stirring. However, the concentration higher than this was only partially dispersed in the solvent. Dispersion ability of DSSF was tested in rest of the solvents at different temperature ranging from room temperature (25 °C) to 120 °C, but none of these were able to disperse the fibers. Hence hydrated TBAH was used as a solvent to disperse DSSF and for the preparation of the magnetic nanocomposite. The stepwise photographic demonstration for the dissolution of DSSF in TBAH and preparation of magnetic nanocomposite is shown in Scheme 1.

Further, to check the role of water in the dissolution process, 40% water was added to all the ILs/DESs shown in Table 1 except TBAH and a similar dissolution process was performed. But none of the ILs/DESs in the presence of water were able to disperse DSSF, even with up to 24 h of treatment (Figure S3). Furthermore, to rule out the basicity of the IL as the reason behind the nanoscale dispersion, we carried out the dissolution experiment with 40% NaOH in place of 40% TBAH in water while maintaining identical the other conditions. After 10 h of continuous stirring at room temperature, the spider silk was found to be partially dispersed in 40% NaOH solution and even after increasing the stirring duration no improvement on dispersion quality was observed (Figure S4). Whereas, only 2 h was required to disperse completely the same amount of DSSF in TBAH. This clearly indicates that the electrostatic interaction present in the IL played a major role in the dispersion of the spider silk fibers.

To check the structural variations of SSF during dissolution and formation of the nanocomposite, the FT-IR spectra of pure SSF, regenerated spider silk fibers from the dispersion in TBAH (RSSF), and the magnetic nanocomposite (SSF−Fe_3O_4) were recorded. The FT-IR absorbance for proteins showed prominent bands in two regions known as amide I and amide II. For pure DSSF, the characteristic IR bands of amide I (C═O stretching vibration) and amide II (C—N stretching vibration) appeared in the ranges of 1620−1700 cm^{-1} and 1500−1580 cm^{-1}, respectively (Figure 2a). The secondary protein structure such as α-helix and β-sheets present in spider silk fibers and the FT-IR band for α-helix and β-sheet was found at 1652 and 1635 cm^{-1}, respectively in the pure DSSF.[31] The bands of SSF observed above appeared intact in the regenerated fibers and in the magnetic nanocomposite, which indicates the amide I and II regions of spider silk were not disturbed during dissolution and nanocomposite formation (Figure 2a). Further, it should be noted that the above characteristic bands of DSSF were masked by the IL bands in the solution prepared in TBAH indicative of participation of the amide I and II regions of SSF in the dissolution process (Figure S5).

The restoration of crystallinity due to the β-sheets of spider silk is important and it should not be disturbed during a dissolution process. The powder XRD of pure DSSF, RSSF, and the magnetic bionanocomposite was recorded, and the results are shown in Figure 2b. As can be seen from the figure, both degummed SSF and regenerated SSF exhibited a sharp peak at $2\theta = 24°$. The sharp peak indicated crystalline nature of the fibers and the crystallinity is observed because of the β-sheet.[10] After preparation of magnetic nanocomposite of SSF with Fe_3O_4, the crystallinity of β-sheet of SSF was found to be disturbed. It should be noted that the sharp peak at 24° was affected during the dissolution in the IL indicative of lost of β-sheet crystallinity of SSF during dissolution (Figure S6). However, as observed above, the crystallinity was restored after regeneration and was lost in the presence of Fe_3O_4. Further, viscosity of DSSF (1 mg/mL in TBAH) was recorded and compared with that of RSSF at the same concentration. Both of the dispersions showed identical viscosity profiles (6.07 cP for DSSF and 6.06 cP for RSSF), indicating similar structural distribution and absence of depolymerization of the proteins during the dispersion process. Because there was a possibility

DOI: 10.1021/acssuschemeng.5b00810
ACS Sustainable Chem. Eng. 2015, 3, 2575−2581

for the presence of a small amount of the IL in the RSSF as an impurity, which was not detected in above experiments and may affect the cytotoxicity and antibacterial efficacy of the material, electrospray ionization-mass spectrometry (ESI-MS) fragmentation of the IPA washings of the materials was performed to detect the IL traces. It was observed that after the first wash, the mass fragmentation of the IL, i.e., m/z 242.4 was visible in the washing (Figure S7) indicating the presence of IL trace in the material. However, no mass fragmentation for the IL was observed in the IPA extract obtained after three consecutive washings (Figure S8) indicating complete removal of the IL traces during the vigorous washing process. Furthermore, the washing of the composite also did not show presence of IL in ESI-MS experiment. The elemental analyses data as shown in Table S2 also indicate the absence of IL trace in the RSSF. These materials were further used for the cytotoxicity and antibacterial assays.

The morphology of the composite material was investigated by FE-SEM and AFM, as shown in Figure 3. The FE-SEM images showed the presence of fibrous spider silk fibers with attachment of Fe_3O_4 particles on the surfaces [Figure 3A,B]. The morphology of Fe_3O_4 particles showed the presence of white colored bulky particles (Figure S9). The presence of Fe on the surface of the spider silk was confirmed by SEM-EDX measurements, which showed the presence of 14.72 at. % of Fe on the surface of the silk (Figure S10). Alignment of the Fe_3O_4 particles on the spider silk fibers was observed in the AFM images [Figure 3C,D].

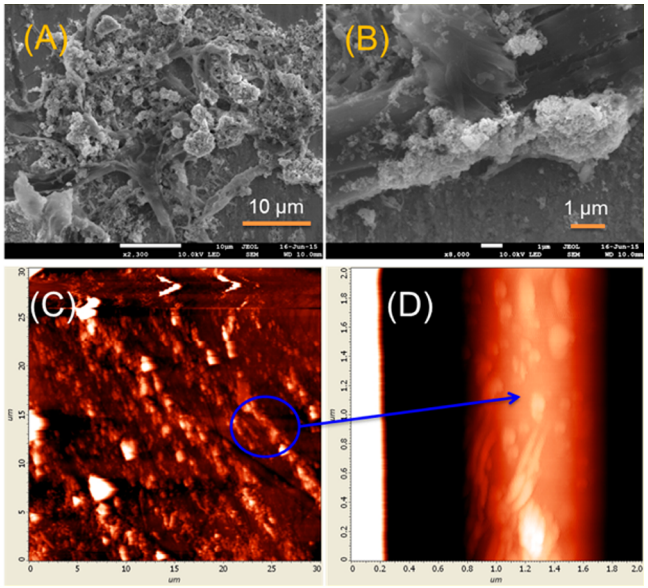

Figure 3. FE-SEM images of SSF−Fe_3O_4 bionanocomposite at (A) low magnification and (B) high magnification and (C and D) AFM images of the bionanocomposite.

Thermogravimetric analyses were performed to investigate the thermal stability of the SSF before and after degumming as well as in the bionanocomposite (Figure 4a). As can be observed from the figure, the minor weight loss (0.6−1.8%) obtained in the temperature range of 30−250 °C due to the bound water present in the materials. This was followed by another mass loss (5.5−9.7%) in the temperature range of 250−300 °C due to the initiation of the degradation of silk protein structure. The major mass loss (27−72%) was obtained within 300−400 °C. The major weight loss indicated that silk protein was degraded due to its unstable random coil structure. In this temperature range, the SSF was degraded to produce H_2, CO, and CO_2 gases. It should be noted that the SSF before and after gumming exhibited almost identical thermal stability (about 70% mass loss in 300−400 °C), whereas the composite showed enhanced thermal stability with about 20% mass loss in the same temperature range. This indicates the iron oxide nanoparticles immensely affect the thermal stability of the silk fibers. The role of the iron oxide nanoparticles in the glass transition temperature (T_g) was also observed in the DSC thermogram. The regenerated SSF had a marginally higher T_g value of 46.5 °C in comparison to that of the fiber before regeneration (42.4 °C). However, the T_g value reduced significantly in the bionanocomposite (38.4 °C), which may be due to the loss of crystallinity due to β-sheets of proteins in the silk fibers (Figure 4b).

Human lung carcinoma (A549) cells have already been evaluated in numerous studies and established as model cell line for identification of the cytotoxic effects of chemical compounds.[32,33] Although the spider silk fibers are already reported as noncytotoxic materials[34] but in order to check influence of IL and the Fe_3O_4 nanoparticles on such properties, both the regenerated spider silk from the IL solution and its magnetic nanocomposite was subjected for the evaluation of cytotoxicity on A549 cell (Figure 5). The percentage viability of cells in spider silk fibers and their nanocomposite with Fe_3O_4 did not show a dose dependent toxicity. Also, on the basis of

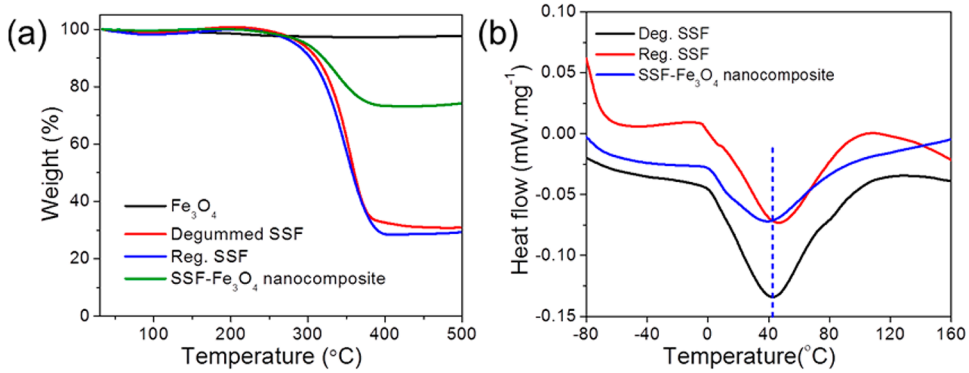

Figure 4. (a) TGA thermogram of Fe_3O_4, degummed SSF, regenerated SSF, and SSF−Fe_3O_4 nanocomposite and (b) DSC of degummed SSF, regenerated SSF, and SSF−Fe_3O_4 nanocomposite.

DOI: 10.1021/acssuschemeng.5b00810
ACS Sustainable Chem. Eng. 2015, 3, 2575−2581

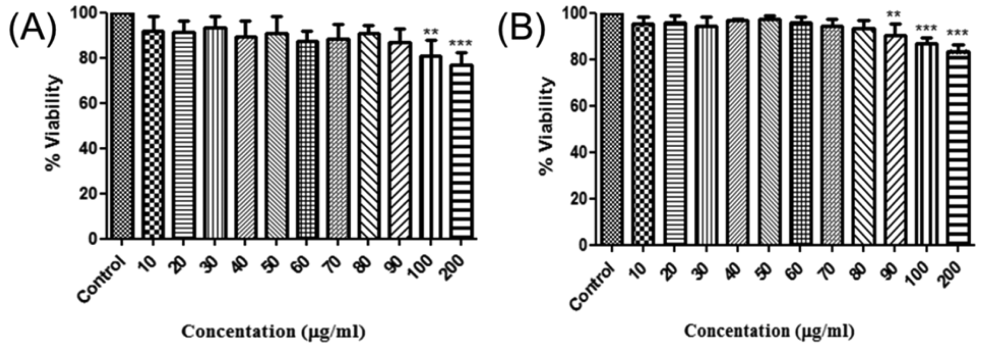

Figure 5. Cytotoxicity study of (A) regenerated degummed spider silk fiber and (B) degummed spider silk fiber–Fe_3O_4 nanocomposite.

the results obtained from the MTT assay, calculations of the IC_{50} values were not possible as the cells did not record 50% cell death in any of the treatment groups including the highest dose. From these observations, it can be concluded that both the compounds were nontoxic in nature when tested against mammalian cells.

Further, spider silk fibers are known to demonstrate antibacterial activities.[35] To check the influence of ionic liquids (dissolution conditions) and the Fe_3O_4 nanoparticles on antibacterial properties, both the regenerated spider silk from the IL solution and its magnetic nanocomposite was subjected for the evaluation of antibacterial properties against both Gram positive and negative bacteria (Figure 6). The antibacterial

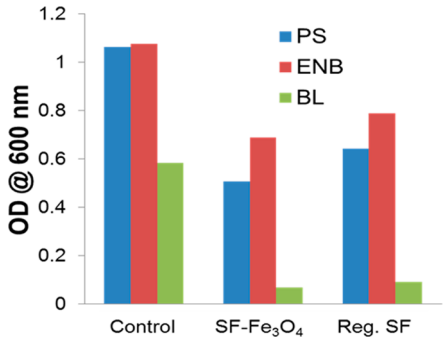

Figure 6. Antibacterial activity of regenerated SSF and the bionanocomposite against different bacteria colonies. *Escherichia coli* (ENB, Gram negative), *Pseudomonas stutzeri* (PS, Gram negative) and *Bacillus licheniformis* (BL, Gram positive).

activity was recorded after 24 h of incubation of test cultures with 20 mg of regenerated spider silk fibers from the IL solution and its magnetic nanocomposite and assessed by comparing the results with control experiment (without the materials). The different bacterial species used for the experiment were *Escherichia coli* (ENB, Gram negative), *Pseudomonas stutzeri* (PS, Gram negative), and *Bacillus licheniformis* (BL, Gram positive). The OD of culture was decreased after loading of 20 mg of regenerated DSF and its magnetic nanocomposite in comparison to control indicating inhibition of bacterial growth in the presence of both the materials. Further, it was observed that although both the materials are antibacterial against both Gram positive and negative bacteria but the nanocomposite has demonstrated superior antibacterial activity in comparison to the degummed spider silk.

Both noncytotoxic and antibacterial properties of the regenerated degummed spider silk indicated that the nanoscale dispersion process of the fibers in ionic liquid had not influenced the cytotoxic and antibacterial properties of the spider silk. Thus, incorporation of magnetic nanoparticles enhanced the antibacterial efficiency of the fibers.

CONCLUSION

Among the various neoteric solvents, hydrated tetrabutylammonium hydroxide was found to disperse 7.5 mg mL^{-1} of spider silk with nanoscale structural distribution at room temperature. Analysis of the regenerated spider silk from the solutions indicated preservation of the chemical structures of the protein blocks in the spider silk. The ionic liquid was used as dispersion media for the fabrication of magnetic nanocomposite. Attachment of Fe_3O_4 nanoparticles on the spider silk surfaces and preservation of the chemical structures of the protein blocks of the spider silk in the composite was also established. Both of the materials do not appear to inhibit the growth of mammalian cells *in vitro* and show antibacterial properties and thus demonstrate their potential for therapeutic applications. The findings further suggest use of quaternary ammonium based ionic liquids as an effective and suitable media for high concentration dispersion of spider silk at room temperature and fabrication of functional composite materials.

ASSOCIATED CONTENT

Supporting Information

The Supporting Information is available free of charge on the ACS Publications website at DOI: 10.1021/acssuschemeng.5b00810.

CHNS data, FT-IR spectra, powder XRD spectra, ESI-MS spectra, SEM images and EDX profile (PDF).

AUTHOR INFORMATION

Corresponding Author

*Dr. Kamalesh Prasad. E-mail: kamlesh@csmcri.org; drkamaleshp@gmail.com. Phone: +91-278 2567760. Fax: +91-278-256756.

Notes

The authors declare no competing financial interest.

ACKNOWLEDGMENTS

K.P. thanks CSIR, New Delhi for the grant of CSIR-Young Scientist Awardees Project and overall financial support. N.S., M.S., and D.M. thank UGC and CSIR for NET-JRF and SRF fellowships and AcSIR for Ph.D. registration. Analytical and centralized instrument facility department of the institute is

DOI: 10.1021/acssuschemeng.5b00810
ACS Sustainable Chem. Eng. 2015, 3, 2575–2581

acknowledged for over all analytical support. This is CSIR-CSMCRI communication No. 130/2015.

REFERENCES

(1) Lintz, E. S.; Scheibel, T. R. Dragline, Egg Stalk and Byssus: A Comparison of Outstanding Protein Fibers and Their Potential for Developing New Materials. *Adv. Funct. Mater.* **2013**, *23*, 4467−4482.
(2) Silva, N. H. C. S.; Vilela, C.; Marrucho, I. M.; Freire, C. S. R.; Neto, C. P.; Silvestre, A. J. D. Protein-based materials: from sources to innovative sustainable materials for biomedical Applications. *J. Mater. Chem. B* **2014**, *2*, 3715−3740.
(3) Kaplan, D. L.; Lombard, S. J.; Muller, W.; Fossey, S. In *Biomaterials: Novel materials from biological sources*; Byrom, D., Ed.; Stockton Press: New York, 1991.
(4) Kaplan, D. L.; Adams, W. W.; Farmer, B.; Viney, C. *Silk Polymers: Material Science and Biotechnology*, 1st ed.; ACS Symposium Series; American Chemical Society: Washington DC, 1994.
(5) Shao, Z.; Vollrath, F. Surprising strength of silk worm. *Nature* **2002**, *418*, 741.
(6) Romer, L.; Scheibel, T. The elaborate structure of spider silk. *Prion* **2008**, *2*, 154−161.
(7) Liu, Y.; Ling, S.; Wang, S.; Chen, X.; Shao, Z. Thixotropic silk nanofibril-based hydrogel with extracellular matrix-like structure. *Biomater. Sci.* **2014**, *2*, 1338−1342.
(8) Schniepp, H. C.; Koebley, S. R.; Vollrath, F. Brown Recluse Spider's Nanometer Scale Ribbons of Stiff Extensible Silk. *Adv. Mater.* **2013**, *25*, 7028−7032.
(9) Porter, D.; Guan, J.; Vollrath, F. Spider silk: Super material or Thin fiber? *Adv. Mater.* **2013**, *25*, 1275−1279.
(10) Astudillo, M. F.; Thalwitz, G.; Vollrath, F. Life cycle assessment of Indian silk. *J. Cleaner Prod.* **2014**, *81*, 158−167.
(11) Zhang, F.; Lu, Q.; Ming, J.; Dou, H.; Liu, Z.; Zuo, B.; Qin, M.; Li, F.; Kaplan, D. L.; Zhang, X. Silk dissolution and regeneration at the nanofibril scale. *J. Mater. Chem. B* **2014**, *2*, 3879−3885.
(12) Zhang, H.; Ma, X.; Cao, C.; Wang, M.; Zhu, Y. Multifunctional iron oxide/silk-fibroin (Fe3O4−SF) composite microspheres for the delivery of cancer therapeutics. *RSC Adv.* **2014**, *4*, 41572−41577.
(13) Mayes, E. L.; Vollrath, F.; Mann, S. Fabrication of Magnetic Spider Silk and Other Silk-Fiber Composites Using Inorganic Nanoparticles. *Adv. Mater.* **1998**, *10*, 801−805.
(14) Sheng, W.; Liu, J.; Liu, S.; Lu, Q.; Kaplan, D. L.; Zhu, H. One-step synthesis of biocompatible magnetite /silk fibroin core−shell nanoparticles. *J. Mater. Chem. B* **2014**, *2*, 7394−7402.
(15) Singh, K. P.; Bae, E. J.; Yu, J. S. Fe−P: A New Class of Electroactive Catalyst for Oxygen Reduction Reaction. *J. Am. Chem. Soc.* **2015**, *137*, 3165−3168.
(16) Wilkes, J. S. A short history of ionic liquids-from molten salts to neoteric solvents. *Green Chem.* **2002**, *4*, 73−80.
(17) Pereira, J. F. B.; Ventura, S. P. M.; e Silva, F. A.; Shahriari, S.; Freire, M. G.; Coutinho, J. A.P. *Sep. Purif. Technol.* **2013**, *113*, 83−89.
(18) Dinis, T. B.V.; Passos, H.; Lima, D. L. D.; Esteves, V. I.; Coutinho, J. A. P.; Freire, M. G. One-step extraction and concentration of estrogens for an adequate monitoring of wastewater using ionic-liquid-based aqueous biphasic systems. *Green Chem.* **2015**, *17*, 2570−2579.
(19) Chen, J.; Vongsanga, K.; Wang, X.; Byrne, N. What Happens during Natural Protein Fibre Dissolution in Ionic Liquids. *Materials* **2014**, *7*, 6158−6168.
(20) Sharma, M.; Mukesh, C.; Mondal, D.; Prasad, K. Dissolution of α-chitin in deep eutectic solvents. *RSC Adv.* **2013**, *3*, 18149−18155.
(21) Mukesh, C.; Mondal, D.; Sharma, M.; Prasad, K. Rapid dissolution of DNA in a novel bio-based ionic liquid with long-term structural and chemical stability: successful recycling of the ionic liquid for reuse in the process. *Chem. Commun.* **2013**, *49*, 6849−6851.
(22) Mondal, D.; Sharma, M.; Mukesh, C.; Gupta, V.; Prasad, K. Improved solubility of DNA in recyclable and reusable bio-based deep eutectic solvents with long-term structural and chemical stability. *Chem. Commun.* **2013**, *49*, 9606−9608.
(23) Phillips, D. M.; Drummy, L. F.; Conrady, D. G.; Fox, D. M.; Naik, R. R.; Stone, M. O.; Trulove, P. C.; De Long, H. C.; Mantz, R. A. Dissolution and Regeneration of Bombyx mori Silk Fibroin Using Ionic Liquids. *J. Am. Chem. Soc.* **2004**, *126*, 14350−14351.
(24) Goujon, N.; Wang, X.; Rajkowa, R.; Byrne, N. Regenerated silk fibroin using protic ionic liquids solvents: towards an all-ionic-liquid process for producing silk with tunable properties. *Chem. Commun.* **2012**, *48*, 1278−1280.
(25) Platnick, N. I. *The world spider catalogue*, version 9.0; American Museum of Natural History: Washington, DC, 2008 (accessed May 12, 2011).
(26) Petkovic, M.; Ferguson, J. L.; Gunaratne, H. Q. N.; Ferreira, R.; Leitão, M. C.; Seddon, K. R.; Rebelo, L. P.; Pereira, C. S. Novel biocompatible cholinium-based ionic liquids−toxicity and biodegradability. *Green Chem.* **2010**, *12*, 643−649.
(27) Abbott, A. P.; Boothby, D.; Capper, G.; Davies, D. L.; Rasheed, R. K. Deep Eutectic Solvents Formed between Choline Chloride and Carboxylic Acids: Versatile Alternatives to Ionic Liquids. *J. Am. Chem. Soc.* **2004**, *126*, 9142−9147.
(28) Kim, S. H.; NAM, Y. S.; Lee, T. S.; Park, W. H. Silk Fibroin Nanofiber. Electrospinning, Properties, and Structure. *Polym. J.* **2003**, *35*, 185−190.
(29) Mondal, D.; Bhatt, J.; Sharma, M.; Chatterjee, S.; Prasad, K. A facile approach to prepare dual functionalized DNA based material in a bio-deep eutectic solvent. *Chem. Commun.* **2014**, *50*, 3989−3992.
(30) Thounaojam, M. C.; Jadeja, R. N.; Valodkar, M.; Nagar, P. S.; Devkar, R. V.; Thakore, S. Oxidative stress induced apoptosis of human lung carcinoma (A549) cells by a novel copper nanorod formulation. *Food Chem. Toxicol.* **2011**, *49*, 2990−2996.
(31) Normandeau, J.; Van Kessel, C.; Nicholson, D.; Routledge, B. R.; Fawcett, A.; Lim-Cole, L.; Condy, C.; Sylvain, N.; Walker, T.; Borondics, F. Spider silk protein structure analysis by FTIR and STXM spectromicroscopy techniques. *Can. Y. Sci. J.* **2014**, *1*, 35−42.
(32) Aufderheide, M.; Knebel, J. W.; Ritter, D. A method for in vitro exposure of human cells to environmental and complex gaseous mixtures: application to various type of atmosphere. *Altern. Lab. Anim.* **2002**, *30*, 433−441.
(33) Carero, A. D. P.; Hoet, P. H. M.; Verschaeve, L.; Schoeters, G.; Nemery, B. Genotoxic effects of carbon black particles, diesel exhaust particles, and urban air particulates and their extracts on a human alveolar epithelial cell line (A549) and a human monocytic cell line (THP-1). *Environ. Mol. Mutagen.* **2001**, *37*, 155−163.
(34) Dams-Kozlowska, H.; Majer, A.; Tomasiewicz, P.; Lozinska, J.; Kaplan, D. L.; Mackiewicz, A. Purification and cytotoxicity of tag-free bioengineered spider silk proteins. *J. Biomed. Mater. Res., Part A* **2013**, *101A*, 456−464.
(35) Wright, S.; Goodacre, S. L. Evidence for antimicrobial activity associated with common house spider silk. *BMC Res. Notes* **2012**, *5*, 326.

DOI: 10.1021/acssuschemeng.5b00810
ACS Sustainable Chem. Eng. 2015, 3, 2575−2581